



UNIVERSITY OF LEEDS

This is a repository copy of *Improved Ionic Conductivity of MgM4P6O24 (M = Hf, Zr) Ceramic Solid-State Electrolytes by Sol-Gel Synthesis*.

White Rose Research Online URL for this paper:
<https://eprints.whiterose.ac.uk/176804/>

Version: Accepted Version

Proceedings Paper:

Adamu, M and Kale, GM orcid.org/0000-0002-3021-5905 (2021) Improved Ionic Conductivity of MgM4P6O24 (M = Hf, Zr) Ceramic Solid-State Electrolytes by Sol-Gel Synthesis. In: ECS Transactions. 239th ECS Meeting: Ionic and Mixed Conducting Ceramics 13 (IMCC 13), 30 May - 03 Jun 2021, Online. Electrochemical Society , pp. 19-27.

<https://doi.org/10.1149/10205.0019ecst>

© 2021 ECS - The Electrochemical Society. This is an author produced version of an article published in ECS Transactions. Uploaded in accordance with the publisher's self-archiving policy.

Reuse

Items deposited in White Rose Research Online are protected by copyright, with all rights reserved unless indicated otherwise. They may be downloaded and/or printed for private study, or other acts as permitted by national copyright laws. The publisher or other rights holders may allow further reproduction and re-use of the full text version. This is indicated by the licence information on the White Rose Research Online record for the item.

Takedown

If you consider content in White Rose Research Online to be in breach of UK law, please notify us by emailing eprints@whiterose.ac.uk including the URL of the record and the reason for the withdrawal request.



eprints@whiterose.ac.uk
<https://eprints.whiterose.ac.uk/>

Improved Ionic Conductivity of $\text{MgM}_4\text{P}_6\text{O}_{24}$ (M = Hf, Zr) Ceramic Solid-State Electrolytes By Sol-Gel Synthesis

Mohammed Adamu^{1,2} and Girish M Kale¹

¹School of Chemical and Process Engineering, University of Leeds, Leeds LS2 9JT, United Kingdom

²Corresponding author: mohammed.adamu@aol.com

Data from electrochemical impedance measurement of $\text{MgHf}_4\text{P}_6\text{O}_{24}$ and $\text{MgZr}_4\text{P}_6\text{O}_{24}$ solid-state electrolytes show significant improvement in the ionic conductivity of the ceramic electrolytes. The electrical behaviour of $\text{MgHf}_4\text{P}_6\text{O}_{24}$ and $\text{MgZr}_4\text{P}_6\text{O}_{24}$ solid-state electrolytes were measured using two-probe analysis at a temperature range of 182 - 764 °C, and at a frequency within 100 mHz to 32 MHz range. In this analysis, promising bulk ionic conductivity of $4.52 \times 10^{-4} \text{ Scm}^{-1}$ and $7.23 \times 10^{-3} \text{ Scm}^{-1}$ were achieved for $\text{MgHf}_4\text{P}_6\text{O}_{24}$ and $\text{MgZr}_4\text{P}_6\text{O}_{24}$ electrolytes, respectively, at impedance maximum temperatures of 747 °C and 725 °C, respectively. The sol-gel method was deployed in the synthesis of $\text{MgHf}_4\text{P}_6\text{O}_{24}$ and $\text{MgZr}_4\text{P}_6\text{O}_{24}$ nanoparticles electrolytes. The thermogravimetric analysis - differential scanning calorimetry (TGA-DSC), and X-ray diffraction (XRD) were characterisation techniques deployed in this study to determine and evaluate the phase composition structure of the nanoparticles calcined at 900 °C and the sample pellets sintered at 1300 °C.

Introduction

Some very impressive data have been published on the sol-gel synthesis technique and how it influences the electrical behaviour of $\text{MgZr}_4\text{P}_6\text{O}_{24}$ solid-state electrolyte (1-8). However, data on sol-gel chemical synthesis of novel $\text{MgHf}_4\text{P}_6\text{O}_{24}$ solid-state electrolyte and other phosphate ceramic electrolytes are scarcely reported.

Recently, notable research interest has been drawn towards further investigation and characterisation of $\text{MgHf}_4\text{P}_6\text{O}_{24}$ and other phosphate ceramic solid-state electrolytes synthesised using the sol-gel chemical route. Consequently, the sol-gel method was deployed in this study for the synthesis of $\text{MgHf}_4\text{P}_6\text{O}_{24}$ and $\text{MgZr}_4\text{P}_6\text{O}_{24}$ electrolytes, and because sol-gel chemical synthesis technique has shown the potential to produce very fine homogeneous powders at a relatively low processing temperature, which can be pelletised and sintered into very dense solid-state electrolytes for application in electrochemical impedance spectroscopy measurement (1,9,10).

Temperature and stoichiometric compositions were some critical factors relied upon while the sol-gel synthesis, calcination and sintering of $\text{MgHf}_4\text{P}_6\text{O}_{24}$ and $\text{MgZr}_4\text{P}_6\text{O}_{24}$ electrolytes into dense sample pellets for impedance measurement were performed.

The sol-gel chemical synthesis technique deployed in this study has brought further improvement in ionic mobility and conductivity of Mg^{2+} -cation conducting species in the ceramic solid-state electrolytes to the open (1,2,9).

In reviewing the ionic conductivity of $\text{MgZr}_4\text{P}_6\text{O}_{24}$ and other phosphates solid-state electrolytes, the data derived from this new study were used to evaluate the impact of sol-gel chemical synthesis on the ionic conductivity of $\text{MgHf}_4\text{P}_6\text{O}_{24}$ and $\text{MgZr}_4\text{P}_6\text{O}_{24}$ electrolytes, and are reported for the first time.

Experimental Procedure

Materials preparation

All chemicals are analytical grade, and used as received without further purification. Pure single phase $\text{MgM}_4\text{P}_6\text{O}_{24}$ ($M = \text{Hf}, \text{Zr}$) solid-state electrolytes were synthesised using sol-gel chemical method to produce very fine nanopowders; this was achieved through mixing on an atomic scale by combining aqueous solutions of precursor soluble salts at relatively low crystallisation temperature and, it produces chemical compositions not always possible by solid-state fusion method. The stoichiometric amount of pure chemical solutions made from the precursors; $\text{Mg}(\text{NO}_3)_2$, ZrOCl_2 and $\text{NH}_4\text{H}_2\text{PO}_4$, to synthesis $\text{MgZr}_4\text{P}_6\text{O}_{24}$ xerogel powders have been reported (1,2). In this new study however, precursors; $\text{Mg}(\text{NO}_3)_2$, HfCl_4 and $\text{NH}_4\text{H}_2\text{PO}_4$, in aqueous form were mixed separately in stoichiometric proportion to synthesis $\text{MgHf}_4\text{P}_6\text{O}_{24}$ xerogel powders. The resulting dried xerogel powders were calcined at $900\text{ }^\circ\text{C}$, then pelletised and sintered at $1300\text{ }^\circ\text{C}$, using data from the TGA-DSC profiles as a guide. Furthermore, the sintered pellets of $\text{MgHf}_4\text{P}_6\text{O}_{24}$ and $\text{MgZr}_4\text{P}_6\text{O}_{24}$ ceramic solid-state electrolytes were further characterised to determine their electrical properties (ionic conductivity). The impedance spectroscopy measurement in this study was achieved using the two-probe analysis at an impedance temperature range from 182 to $764\text{ }^\circ\text{C}$ and at a frequency range within 100 mHz to 32 MHz .

Materials characterisation

The STA 8000 (PerkinElmer, Seer Green, UK) was used to measure the TGA-DSC, which was later used to analyse the weight loss and thermal oxidation behaviour of

the dried xerogel powders. In this measurement, effective optimisation calcination condition of the xerogel powders in a controlled atmosphere at a flow rate of 50 mL min^{-1} using a constant heating-cooling rate at $10 \text{ }^\circ\text{C min}^{-1}$ within a temperature range of $30 - 1000 \text{ }^\circ\text{C}$, akin to that described in our recent papers (2,9) was established. Based on the data from this measurement, the resultant dried xerogel powders were calcined at $900 \text{ }^\circ\text{C}$, and the calcined nanopowders were pelletised and later sintered at $1300 \text{ }^\circ\text{C}$, using the same heating-cooling condition.

Powder x-ray diffractometer (Bruker D8 advance, Karlsruhe, GmbH) equipped with $\text{CuK}\alpha_1$ ($\lambda = 1.5406 \text{ \AA}$) radiation source operating at 30 kV and 45 mA , and calibrated against Si standard was deployed to analyse the phase structure of $\text{MgHf}_4\text{P}_6\text{O}_{24}$ and $\text{MgZr}_4\text{P}_6\text{O}_{24}$ electrolytes. XRD data was collected over $10^\circ \leq 2\theta \leq 80^\circ$ scan range.

Impedance analyser, Solartron SI1260 FRA (Hampshire, UK) was used to analyse the electrical properties of the solid-state electrolytes in this study. Sintered pellets of $\text{MgHf}_4\text{P}_6\text{O}_{24}$ and $\text{MgZr}_4\text{P}_6\text{O}_{24}$ solid-state electrolytes were mildly ground to achieve a flat surface area without diminishing the pellets thickness. Platinum paste (Sigma-Aldrich, UK) was lightly applied to the opposite parallel faces of the sintered pellets, and then allowed to dry before firing in a tube furnace (Fig. 1) at $800 \text{ }^\circ\text{C}$ for 0.5 h to form contact electrodes on both surfaces of the pellets. Electrical conductivity was therefore recorded as a function of temperature and frequency in the temperature range from 182 to $764 \text{ }^\circ\text{C}$ and frequency range from 100 mHz to 32 MHz .

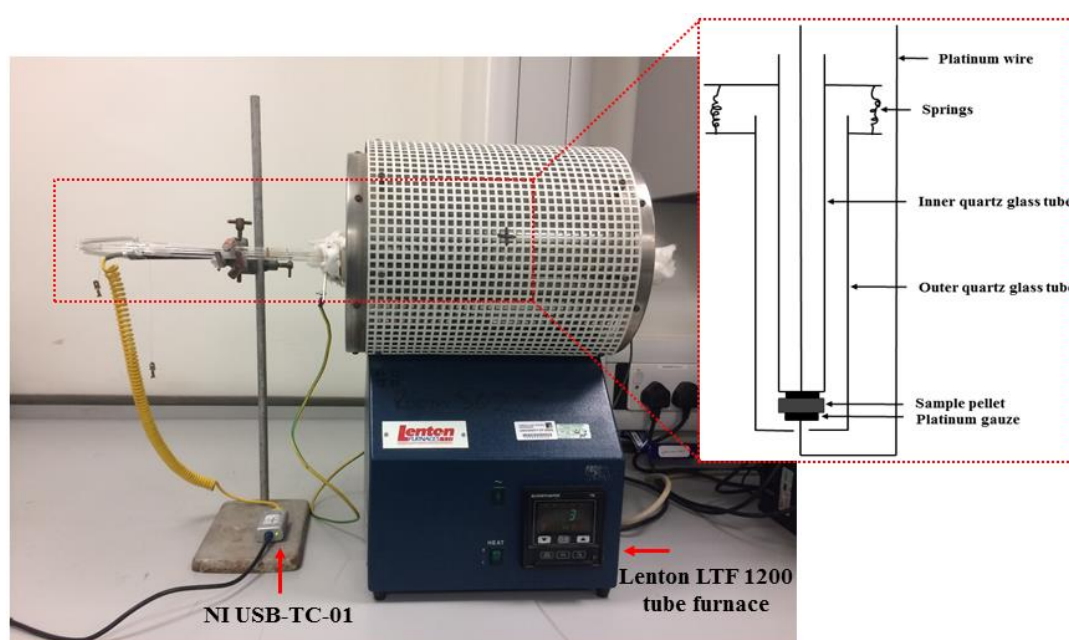


Figure 1. Quartz assembly rig for impedance measurements in a Lenton LTF 1200 tube furnace (1,2,9)

Results and Discussions

Thermal analysis (TGA-DSC)

Thermal stability of $\text{MgZr}_4\text{P}_6\text{O}_{24}$ ceramic solid-state electrolyte was reported in our previous papers (1,2). However, the thermal analysis (TGA-DSC) profile curves in Fig. 2 shows the main decomposition changes in the $\text{MgHf}_4\text{P}_6\text{O}_{24}$ xerogel powders. The TGA decomposition changes in this study is presented in three different regions: The first region within 30 - 100 °C corresponds to the removal of lattice H_2O . The weight loss in the 150 - 500 °C temperature region is because of the decomposition or oxidation of gelled inorganic precursor materials such as $\text{Mg}(\text{NO}_3)_2$, HfCl_4 and $\text{NH}_4\text{H}_2\text{PO}_4$. There was no further reduction in weight above 500 ± 25 °C for the $\text{MgHf}_4\text{P}_6\text{O}_{24}$ xerogel powders. Similarly, the DSC profiles of $\text{MgHf}_4\text{P}_6\text{O}_{24}$ xerogel powders in Fig. 2 shows clearly two endothermic decomposition peaks at 150 °C and 350 °C, and an exothermic peak at 900 °C. It is therefore known that the inorganic precursor, $\text{NH}_4\text{H}_2\text{PO}_4$ decomposes into $(\text{NH}_4)_3\text{H}_2\text{P}_3\text{O}_{10}$ and H_2O molecules at 140 - 170 °C which could be responsible for the endothermic peak at 150 °C. $\text{Mg}(\text{NO}_3)_2$ compound also decomposes into MgO , NO_2 , and O_2 at a temperature above 300 °C, this could be responsible for the endothermic peak at 350 °C. The reactive oxide HfO_2 formed by oxidation of HfCl_4 at 432 °C yields $\text{MgHf}_4\text{P}_6\text{O}_{24}$ after stoichiometric composition reaction with MgO and P_2O_5 reactive oxides at a temperature of 900 °C. Therefore, the exothermic peak observed at 900 °C indicates the formation of a single phase $\text{MgHf}_4\text{P}_6\text{O}_{24}$ nanoparticles with full crystallinity. In this study however, the TGA-DSC measurement was limited to 1000 °C because of the heating capacity range of the equipment.

Based on the TGA-DSC data reported for $\text{MgZr}_4\text{P}_6\text{O}_{24}$ xerogel powders (1,2) and for $\text{MgHf}_4\text{P}_6\text{O}_{24}$ xerogel powders reported in this study (Fig. 2), it was resolved that a pure single phase of the respective solid-state electrolytes was formed at 800 °C and fully crystallised at 900 °C.

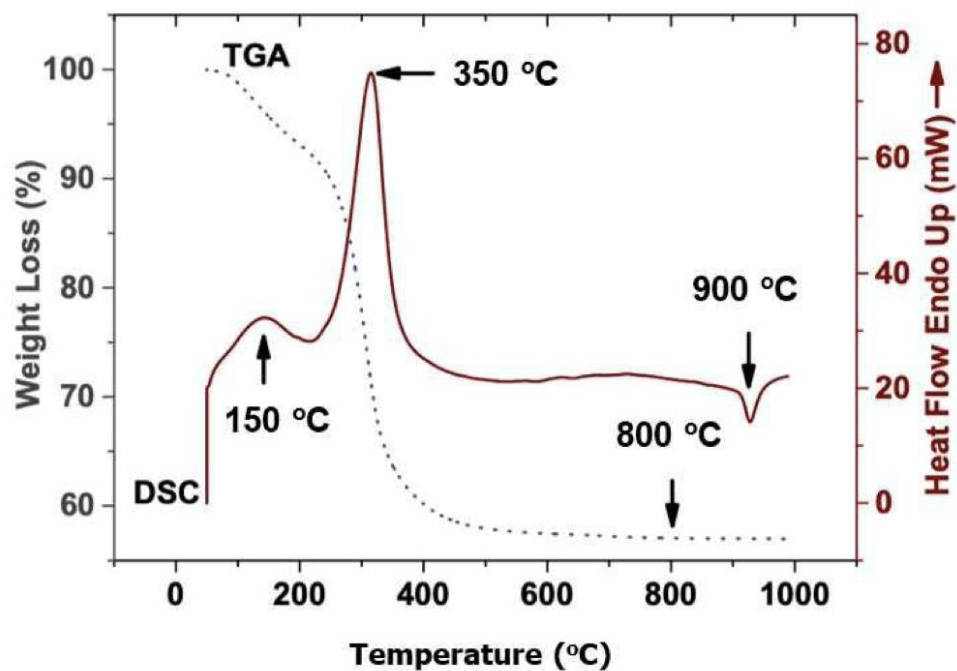


Figure 2. TGA-DSC profile curves of $\text{MgHf}_4\text{P}_6\text{O}_{24}$ dried xerogel powders with a scan rate of $10^\circ\text{C min}^{-1}$ in the air (9).

Phase identification (XRD)

X-ray diffraction data of calcined and sintered $\text{MgZr}_4\text{P}_6\text{O}_{24}$ nanoparticles solid-state electrolyte has been published (1,2). Furthermore, XRD peaks of $\text{MgHf}_4\text{P}_6\text{O}_{24}$ solid-state electrolyte presented in Fig. 3 also corroborated the conclusion arrived at using Fig. 2, which shows a single phase formation for the dried xerogel powders calcined at 900°C and the corresponding pelletised nanopowders, sintered at 1300°C , with majority of the peaks matched and indexed appropriately.

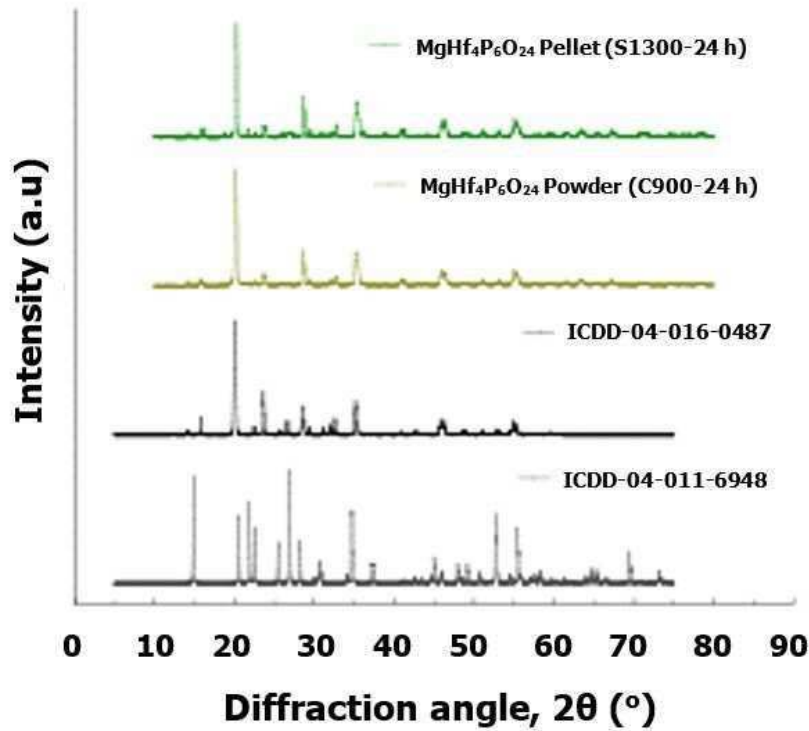


Figure 3. X-ray diffraction peaks of $\text{MgHf}_4\text{P}_6\text{O}_{24}$ nanopowders calcined at 900 °C and sample pellets sintered at 1300 °C. All the peaks were indexed to $\text{Mg}_{0.5}\text{Zr}_2(\text{PO}_4)_3$ [ICDD-04-016-0487] and $\text{Zr}_2(\text{PO}_4)_2\text{O}$ [ICDD-04-011-6948] (9).

Temperature dependence of ionic conductivity

Ionic conductivity of $\text{MgM}_4\text{P}_6\text{O}_{24}$ ($M = \text{Hf}, \text{Zr}$) solid-state electrolytes as a function of temperature is presented in Fig. 4. In this study, ionic conductivity of $\text{MgHf}_4\text{P}_6\text{O}_{24}$ and $\text{MgZr}_4\text{P}_6\text{O}_{24}$ solid-state electrolytes were measured and evaluated. However, in Fig. 4, several points are outlined: Firstly, the linearity of the plots suggest there are no significant structural and phase decomposition changes noticed in the impedance temperature range. This further identifies $\text{MgHf}_4\text{P}_6\text{O}_{24}$ and $\text{MgZr}_4\text{P}_6\text{O}_{24}$ solid-state electrolytes as having comparable ionic conducting species. In this study, activation energy, E_a which includes energy of formation and migration of ions in $\text{MgHf}_4\text{P}_6\text{O}_{24}$ and $\text{MgZr}_4\text{P}_6\text{O}_{24}$ ceramic solid-state electrolytes were determined from the gradient of Arrhenius plots by fitting the ionic conductivity data measured in this study with Arrhenius equation presented in Eq. 1.

$$\sigma_T = \sigma_0(T) \exp\left(-\frac{E_a}{kT}\right) \quad [1]$$

where σ_0 is pre-exponential factor related to the effective number of mobile charge carriers, E_a is the thermal activation energy for oxide ion migration, T is absolute temperature (in Kelvin, K) and k is Boltzmann constant.

Ionic conduction is a thermally activated transport process, this implies that the ionic conductivity of a solid-state electrolyte increases at increasing temperatures (11-13). In this study however, the ionic conductivity of $\text{MgHf}_4\text{P}_6\text{O}_{24}$ and $\text{MgZr}_4\text{P}_6\text{O}_{24}$ solid-state electrolytes increases exponentially as temperatures increases. Meanwhile, the respective ionic conductivity of $\text{MgHf}_4\text{P}_6\text{O}_{24}$ and $\text{MgZr}_4\text{P}_6\text{O}_{24}$ solid-state electrolytes deduced from Fig. 4 are $4.52 \times 10^{-4} \text{ Scm}^{-1}$ at $747 \text{ }^\circ\text{C}$ and $7.23 \times 10^{-3} \text{ Scm}^{-1}$ at $725 \text{ }^\circ\text{C}$, respectively. However, the activation energy, E_a of $\text{MgHf}_4\text{P}_6\text{O}_{24}$ and $\text{MgZr}_4\text{P}_6\text{O}_{24}$ solid-state electrolytes deduced from the slope of $\ln\sigma_{dc}T - 1000T^{-1}$ plots in Fig. 4 are $0.74 \pm 0.02 \text{ eV}$ and $0.84 \pm 0.04 \text{ eV}$, respectively. This therefore shows that $\text{MgHf}_4\text{P}_6\text{O}_{24}$ solid-state electrolyte with lower $E_a = 0.74 \pm 0.02 \text{ eV}$ has a higher mobility of Mg^{2+} -cations but exhibit a lower conductivity ($\sigma_{ac} = 4.52 \times 10^{-4} \text{ Scm}^{-1}$) at $747 \text{ }^\circ\text{C}$ while $\text{MgZr}_4\text{P}_6\text{O}_{24}$ solid-state electrolyte with higher $E_a = 0.84 \pm 0.04 \text{ eV}$ exhibits a higher conductivity ($\sigma_{ac} = 7.23 \times 10^{-3} \text{ Scm}^{-1}$) at $725 \text{ }^\circ\text{C}$. The conductivity data of both solid-state electrolytes in Fig. 4 shows that the $\text{MgZr}_4\text{P}_6\text{O}_{24}$ electrolyte measured between $197 - 725 \text{ }^\circ\text{C}$ has a better ionic conducting specie than the $\text{MgHf}_4\text{P}_6\text{O}_{24}$ solid-state electrolyte measured between $182 - 747 \text{ }^\circ\text{C}$. However, the $\text{MgHf}_4\text{P}_6\text{O}_{24}$ solid-state electrolyte remains chemically more stable at higher temperatures than $\text{MgZr}_4\text{P}_6\text{O}_{24}$ solid-state electrolyte (1).

Furthermore, it was observed that the crossover point in Fig. 4 for the bulk ionic conductivity is identified at $394 \text{ }^\circ\text{C}$. This suggest that $\text{MgZr}_4\text{P}_6\text{O}_{24}$ electrolyte is a marginally better ionic conductor than $\text{MgHf}_4\text{P}_6\text{O}_{24}$ electrolyte at temperatures greater than $394 \text{ }^\circ\text{C}$ whereas, at temperatures below $394 \text{ }^\circ\text{C}$, $\text{MgHf}_4\text{P}_6\text{O}_{24}$ electrolyte is marginally better than $\text{MgZr}_4\text{P}_6\text{O}_{24}$ electrolyte. This observation could be due to the enhancement of ionic conductivity owing to space-charge region effect (14) since the

MgZr₄P₆O₂₄ electrolyte is a composite electrolyte while, MgHf₄P₆O₂₄ is a single phase solid-state electrolyte.

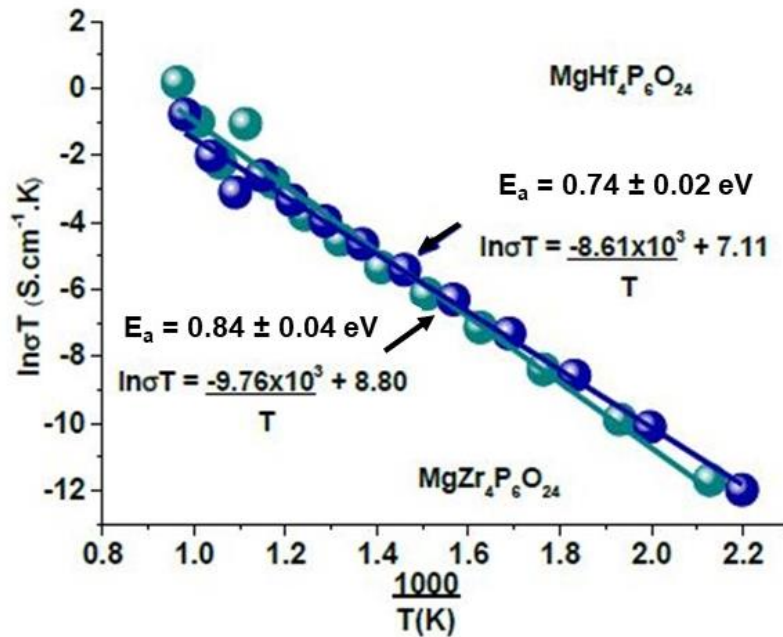


Figure 4. Bulk ionic conductivity profiles of MgZr₄P₆O₂₄ and MgHf₄P₆O₂₄ solid-state electrolytes as a function of temperature (1,2,9)

Conclusion

In relying on the data extracted from TGA-DSC profiles, ground xerogel powders of MgZr₄P₆O₂₄ and MgHf₄P₆O₂₄ solid-state electrolytes were calcined and then sintered at temperatures of $900 \leq T \leq 1300$, respectively. Whereas, chemical stability and structural orientation (phase formation) were identified using thermal analysis, XRD technique was deployed to corroborate the formation of a single phase MgZr₄P₆O₂₄ and MgHf₄P₆O₂₄ solid-state electrolytes, calcined and sintered at $900 \leq T \leq 1300$, respectively. While the ionic conductivity data of MgZr₄P₆O₂₄ solid-state electrolyte have been published, the ionic conductivity of MgHf₄P₆O₂₄ electrolyte published in this study for the first time evaluates the claim that MgZr₄P₆O₂₄ is a better solid-state ionic conductor.

Acknowledgements

This research material is based entirely upon my PhD findings, and as such, we wish to sincerely thank all those who were directly or indirectly involved in it.

References

- (1) M. Adamu and G.M. Kale, *J. Phys. Chem. C*. **120(32)**, 17909-17915 (2016).
- (2) M. Adamu, K.T. Jacob and G.M. Kale, *J. Electrochem. Soc.* **167**, 027532 (2020).
- (3) G.M. Kale, L. Wang and Y. Hong, *Int. J. Appl. Ceram. Technol.* **1(2)**, 180-187 (2004).
- (4) J.W. Fergus, *Electrochemical sensors: Fundamentals, Key Materials, and Applications. Solid State Electrochemistry I: Fundamentals, Materials and their Applications.* (2009) 427-491.
- (5) V.I. Pet'kov, A.S. Shipilov, A.V. Markin and N.N. Smirnova, *J. Therm. Anal. Calorim.* **115(2)**, 1453-1463 (2014).
- (6) G.M. Kale and K.T. Jacob, *J. Mater. Res.* **4(2)**, 417-422 (1989).
- (7) G.M. Kale, A.J. Davidson and D.J. Fray, *Solid State Ionics.* **86-88**, 1107-1110 (1996).
- (8) S. Mudenda and G.M. Kale, *Electrochimica Acta.* **258**, 1059-1063 (2017).
- (9) M. Adamu and G.M. Kale, *ECS Trans.* **98(12)**, 17-38 (2020).
- (10) M. Kakihana, *J. Sol-Gel Sci Technol.* **6(1)**, 7-55 (1996).
- (11) M.G. Bellino, D.G. Lamas and N.E. Walsoe de Reza, *Adv. Mater.* **18(22)**, 3005-3009 (2006).
- (12) M. Prabu, S. Selvasekarapandian, A.R. Kulkarni, S. Karthikeyan, G. Hirankumar and C. Sanjeeviraja, *Solid State Ionics.* **13(9)**, 1714-1718 (2011).
- (113) A. Zuttel, *Mater. Today.* **6(9)**, 24-33 (2003).
- (14) N. Vaidehi, R. Akila, A.K. Shukla and K.T. Jacob, *Mat. Res. Bull.* **21(8)**, 909-916 (1986).